Effects of large-scale structures on inner layer in high Reynolds number turbulent channel flow

Yoshinobu Yamamoto
Department of Mechanical Engineering
University of Yamanashi
4-3-11, Takeda, Kofu, 400-8511, Japan
yamamotoy@yamanashi.ac.jp

Yoshiyuki Tsuji
Department of Energy Science and Engineering
Nagoya University
Furo, Chikusa, Nagoya, 464-8601, Japan
c42406a@nucc.cc.nagoya-u.ac.jp

ABSTRACT

Direct numerical simulations of turbulent channel flows up to Re_τ =8000 were carried out. Present resolution of DNS database ensures over twice fine resolution of Kolmogorov wave length at all wall-normal heights. In case of Re_τ = 8000, 8640 (Δx^+=14.8), 4096 (Δy^+=0.6-8.0), and 6144 (Δz^+=8.3) grid points (resolutions in wall-units) were adapted for stream, wall-normal, and spanwise directions, respectively. As the results, a logarithmic profile of the mean velocity and a second peak of the production/dissipation rate of the turbulent energy were clearly observed for Re_τ > 4000. The second peak of pre-multiplied spectrum at overlap regions in streamwise turbulent velocity was appeared in cases of Re_τ = 4000 and 8000. The wave-length of this second peak is almost $5h$, where, h is channel-half height. In this overlap region, $90 < y+ < 200$, the formation of the intermediate scale structures between large-scale structures and primary structures near the wall were visually observed. The characteristics of these intermediate scale structures might be regarded as the high-Reynolds number effects.

INTRODUCTION

Characteristics of high-Reynolds number wall-bounded turbulence have been suggested by theoretical and experimental studied. Especially, interactions between large-scale structures on a logarithmic region proposed by Huchins & Marusics (2007) are interesting and well explain that the inner-scaled peak in the stream-wise turbulent intensity increases with Reynolds number. The remarkable features such as the second-peak in the pre-multiplied spectrum were observed in the friction Reynolds number (Re_τ) 7,300. Recently, direct numerical simulations (DNS) of channel flows with $Re_\tau \approx 4000$ were performed by Lozano-Dur´an & Jim´enez (2014) and Bernardini et al. (2014). More recently, Lee & Moser (2015) performed for $Re_\tau \approx 5200$. However, some differences such as the von Karman constant distributions between $Re_\tau \approx 4000$ and $Re_\tau \approx 5200$ are reported by Lee & Moser (2015).

In this study, we have developed the large-scale direct numerical simulation (DNS) code of turbulent channel flows based on the high-order accuracy finite difference scheme. Using our DNS code, the DNS database up to Re_τ =8000 can be obtained, and we investigate the interactions between large-scale structures on a logarithmic region.

DNS F

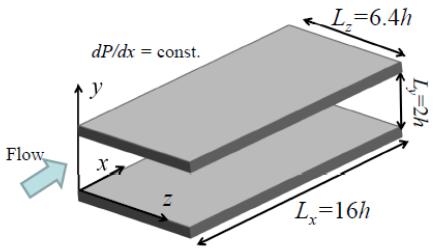

FIG.1. Computational domain and coordinate system.

As shown in Fig. 1, the target flow is assumed to be a fully developed turbulent channel flow driven by the constant mean pressure gradient in the streamwise direction. DNSs of the incompressible Navier–Stokes equation are conducted by the 10th-order accuracy Finite Difference Method (FDM) proposed by Morinishi et al. (1998) for the stream- and spanwise directions, and the second-order FDM for the wall-normal direction. To detect the wavelength of the second-peak in the pre-multiplied spectrum measured by Hutchins & Marusic (2007), which is corresponded to 6δ, where δ is the boundary layer thickness, the computational domain size in all cases is adapted $16h \times 2h \times 6.4h$ for the streamwise (x), wall-normal (y), and spanwise (z) directions, respectively, where h is the channel half width.

In a fully developed channel flow, the kinematic energy balance integral over the channel cross section is given by Eq. (1),

$$0 = U_b^+ - \underbrace{\int_0^{h^+} \left(\frac{\partial U^+}{\partial y^+} \right)^2 dy^+}_{E} - \underbrace{\int_0^{h^+} \varepsilon^+ dy^+}_{E_T} \quad . \tag{1}$$

Here, U_b is the bulk mean velocity, U is the streamwise mean velocity, ε is the turbulent energy dissipation rate, and the superscript + denotes non-dimensional quantities normalized by friction velocity (u_τ) and kinematic viscosity (ν). The second term (E) on the right side in Eq. (1) is the energy dissipation by the mean velocity and the third term (E_T) is the energy dissipation by the turbulence. Laadhari (2007) reports that E_T is greater than E for the friction Reynolds number ($\mathrm{Re}_\tau = u_\tau h/\nu$) > 500. Accordingly, present DNS starts from Re_τ = 500 up to 8000. Present DNS conditions are tabled in Table 1, where T denotes the time-integration length to obtain the turbulent statistics, and Δx, Δy, Δz are the grid resolutions for the streamwise, wall-normal, and spanwise directions, respectively. In case of Re_t =8000, time integration length: T^+/Re_τ =6.3 is correspond to 10 wash-out times, where a wash-out is defined as the time taken by a fluid particle at the centreline to cross the computational box ; L_x=16h.

Figure 2 shows the wall-normal grid resolution in case of Re_τ = 4000. Notes that l_K is the Kolmogorov length and resolutions of Re_τ = 4200; Lozano-Duran & Jimenez (2014), Re_τ = 4079; Bernadini et al. (2014) and Re_τ = 5200; Lee & Moser (2015) were also plotted in Fig.2. Present resolution ensures over twice fine resolution of Kolmogorov wave length at all wall-normal heights. In case of Re_τ = 8000, DNS in 8640×4096×6144 grid points for stream, wall-noraml and spanwise directions was carried out by using the two-types of Peta-scale supercomputer systems. One is a vector-parallel supercomputer system; NEC SX-ACE/1024nodes at the Cyber Science Center, Tohoku University and Japan Agency for Marin-Earth Science and Technology (JAMSTEC). The other is the Plasma Simulator; Fujitsu FX100/2048nodes at National Institutes for Fusion Science (NIFS). Elapse time per each time-step is 6.6 s and 3.6 s by using SX-ACE/1024nodes and FX100/2048nodes, respectively.

Table 1. DNS conditions.

Re_τ	Δx^+	Δy^+	Δz^+	T^+/Re_τ	U_b^+	E_T
500	9.3	0.2-5.3	6.3	13.1	18.22	9.06
1000	11.1	0.3-8.0	8.3	12.0	19.92	10.94
2000	11.1	0.3-8.0	8.3	10.0	21.74	12.76
4000	11.1	0.3-8.0	8.3	9.0	23.27	14.29
8000	14.8	0.3-8.0	8.3	6.3	24.97	16.30

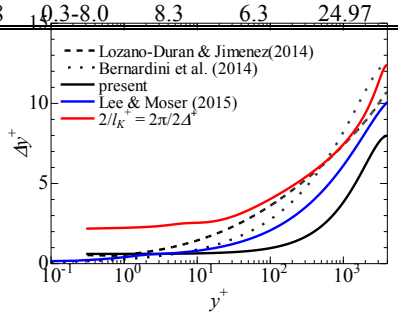

FIG.2. Wall-normal grid resolution in case of Re_τ =4000.

VALIDATION OF PRESENT DNS DATABASE

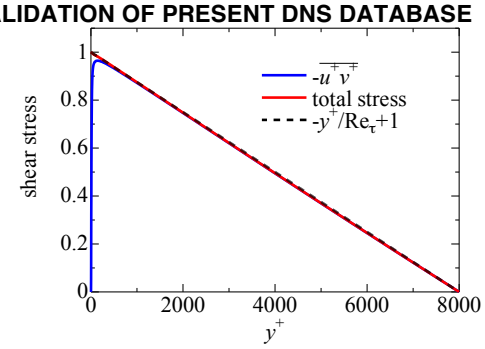

FIG.3 Total shear stress profiles in case of Re_τ =8000.

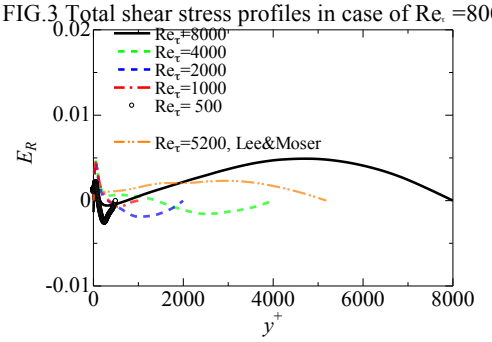

FIG.4 Residual in shear stress balance in all cases.

In steady-state fully developed channel flow, the total shear stress shows a liner profile as function of wall-normal height (y) as follow;

$$1 - \frac{y^+}{\mathrm{Re}_\tau} = -\overline{u^+v^+} + \frac{dU^+}{dy^+} \quad . \tag{2}$$

Here, $-\overline{u^+v^+}$ denotes Reynolds shear stress. To check statistical errors in DNS data, Tompson et al. (2016) used the following residual in shear stress balance;

$$E_R(y^+) = 1 - \frac{y^+}{\mathrm{Re}_\tau} + \overline{u^+v^+} - \frac{dU^+}{dy^+} \quad . \tag{3}$$

Figure 3 shows the shear stress profiles in case of Re_τ =8000, and residuals (E_R) in all cases are shown in FIG.4. We can confirm that the total shear stress profile in case of Re_τ =8000 shows a liner profile and the residuals of present DNS database is less than 0.05. For these results, time integration lengths of present DNS database can be considered larger than the least length to obtain the fully developed status.

The adequacy of the grid resolution used for the present DNSs has been verified through a grid sensitivity study carried out at Re_τ =1000, for reasons of computational feasibility. The grid sensitivity for the streamwise pre-multiplied spectrum in case of Re_τ=1000 are shown in FIG.5, here the DNS result by a hybrid code of Fourier spectral method for x and z directions and second order accuracy FDM for y direction, Yamamoto & Kunugi (2016) was used as the reference data. The resolution in FIG.5-(a) is as same as in cases of Re_τ =2000 and 4000 in present DNS database,

and one in FIG.5-(b) is as same as in case of Re_τ =8000. In this study, the streamwise energy spectrum; E_{uu} is defined by

$$\overline{uu} = \int_0^\infty E_{uu} dk_x \quad . \tag{4}$$

Here, k_x is the streamwise wave-number. Any difference caused by the grid resolution can't be observed, and both results by present FDM code are in good agreements with the result by spectral method.

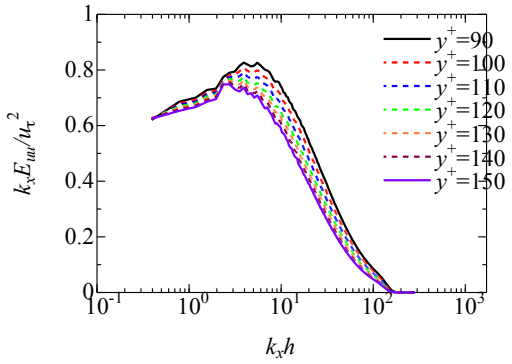

(a)

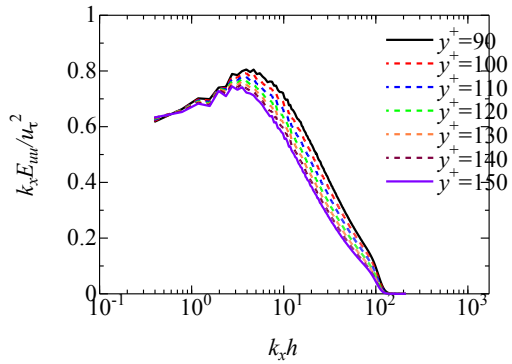

(b)

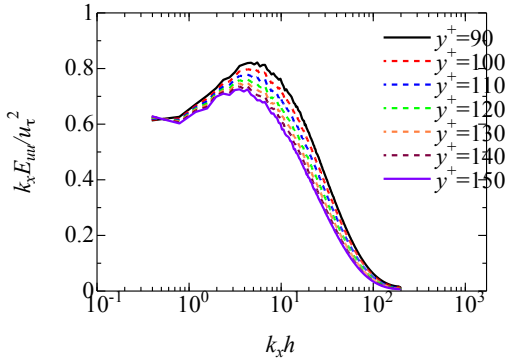

(c)

FIG.5 Grid sensitivity for the streamwise pre-multiplied spectrum in case of Re_τ=1000, (a) Δx^+=11.1, Δy^+=0.6-8.0, Δz^+=8.3 by preset FDM code, (b) Δx^+=14.8, Δy^+=0.6-8.0, Δz^+=8.3 by preset FDM code, and (c) Δx^+=12.0, Δy^+=0.6-8.0, Δz^+=8.3 by a hybrid Fouries spectral (x and z) and 2nd FDM (y) code.

RESULTS

Von Karman constant

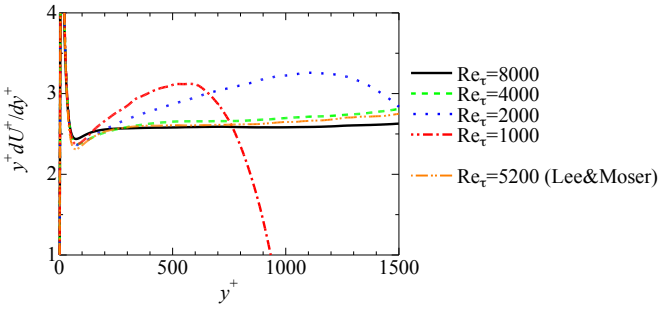

FIG.6 Distribution of indicator function.

Figure 6 shows the indicator function β ($=y^+dU^+/dy^+$). The profile in 5200 by Lee & Moser (2015) is also plotted in FIG.6. Lee & Moser (2015) shows that the indicate function of Re_τ = 5200 has a plateau profile between y^+ = 300 and y/h = 0.15. The profile of Re_τ=4000 is in good agreement with Lee & Moser (2015), though it is a little low-Reynolds number. The profile of Re_τ = 8000 also shows the constant value; β = 2.6 between y^+ = 300 and y/h = 0.15 (y^+=1200).

Streamwise turbulent intensity

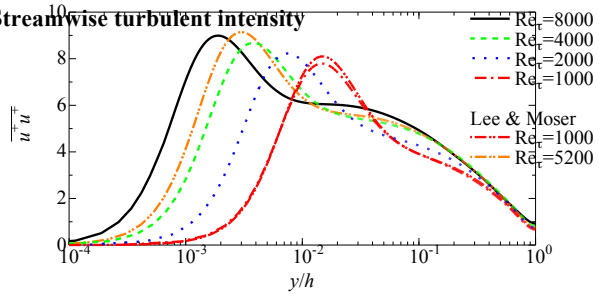

FIG.7 Variance of streamwise turbulence as a function of y/h.

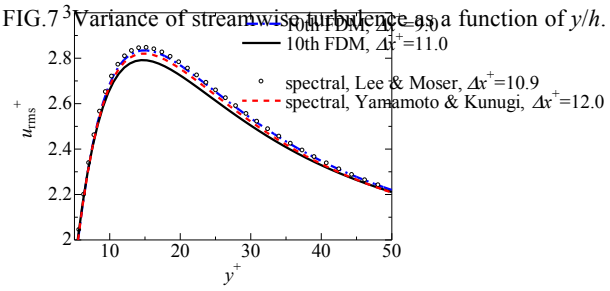

FIG. 8 Comparison of streamwise turbulent intensity near peak region in case of Re_τ =1000.

Figure 7 shows the variance of streamwise turbulence as a function of y/h. The results of Re_τ=1000 and 5200 by Lee & Moser (2015) are also plotted in FIG.7. Townsend's attached eddy hypothesis (Townsend 1980) implies that in the high Reynolds number limit, logarithmic variation of the streamwise velocity variance. There are no clear range of logarithmic variation in case of Re_τ =8000. However, the plateau region from

y/h =0.01 to 0.03 can be observed in case of Re_τ =8000. To comparison with results by Lee & Moser (2015), present results show the underestimation of the peak value. To obtain the quantitative agreements in the peak value of streamwise variance, the present 10th FDM code needs to use the higher resolution; Δx^+=9.0 as shown in FIG.8. Besides, this underaestimation tendency of present DNS database can be observed only in 10 < y^+ < 40, and quantitative agreements with spectral data by Lee & Moser (2015) and Yamamoto & Kunugi (2017) are confirmed in other wall-normal heights.

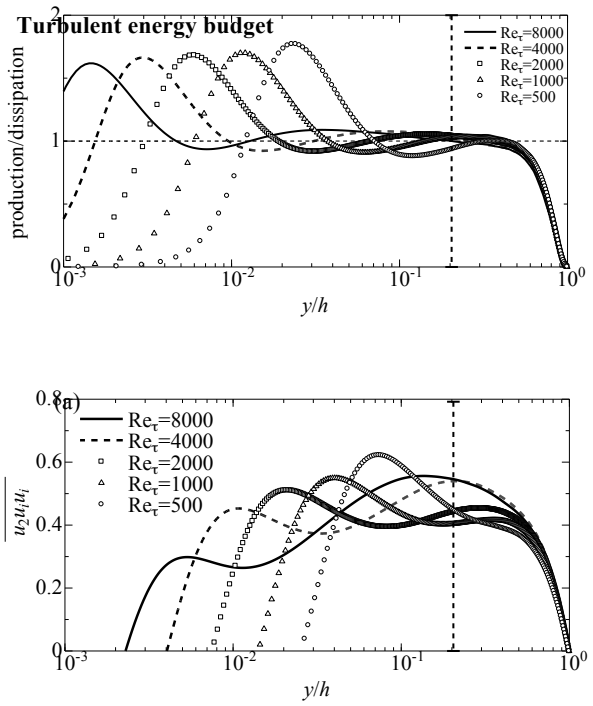

(b)

FIG. 9 Reynolds number effects on turbulent energy budget; (a) the ratio of production and dissipation rate, and (b) triple correlation of turbulent diffusion term.

Reynolds number effects on turbulent kinetic energy budget are appeared in the ratio of production and dissipation rate, and the triple correlation of turbulent disunion term as shown in FIG.9.

Figure 9-(a) shows the ratio of production and dissipation rate of turbulent kinetic energy. The peak value of the 1st peak at the buffer region are slightly decreased with increasing of Re_τ. The reason is why the dissipation rate is increased with increasing of Re_τ, but the production at this wall-normal heigh is almost constant for Re_τ > 1000. As well as results of Bernadini et al. (2014) and Lee & Moser (2015), the other region in which production exceeds dissipation can be observed from y/h <0.2 for Re_τ > 1000, and this region is larger with increasing of Re_τ. These results show that the increasing of the streamwise turbulent intensity with increasing of Re_τ will be caused by the turbulent production far from wall-region at y/h < 0.2.

The remarkable change at this wall-normal height at y/h = 0.2 can be observed in the triple correlation of turbulent diffusion term in turbulent kinetic energy for Re_τ> 4000. In case of Re_τ> 2000, the profiles of triple correlation have the two peaks as shown in FIG.9-(b). The appearance of the second peak is reported by Hoya & Jimenez (2008) for Re_τ =2000. In case of Re_τ > 4000, the magnitude of second peak at y/h =0.2 exceeds of the fist peak. This indicates that energy flows through the turbulent diffusion toward the wall and turns toward the channel center at the boundary; y/h =0.2.

Pre-multiplied spectrum

Figure 10 shows the pre-multiplied spectrum of streamwise turbulent velocity at overlap region; 90 < y^+ < 150.

In case of Re_τ =1000 as shown in FIG.10-(a), there is one peak in which wave-length; λ_x^+ is almost 1300 in wall-units ($k_x h$≈ 4.7).

In case of Re_τ =2000 as shown in FIG.10-(b), the second peak in which wave-length; λ_x is almost 5.2h ($k_x h$≈ 1.2) is appeared, and the wave-length of the first peak is 1461 in wall-units. ($k_x h$≈ 8.6).

In case of Re_τ =4000 as shown in FIG.10-(c), the second peak is changed into the bimodal peaks and the magnitude of the second peaks are increased. The wave-length of the larger second peak is almost 5.4h ($k_x h$≈ 1.2). The plateau region corresponded to the k_x^{-1} law proposed by Perry et al. (1982) is existed for 3 < $k_x h$ < 7. The magnitude of the pre-multiplied spectrum at the plateau region is in good agreement with the value 0.8 of boundary layers (Nickels et al. 2005) and channel (Lee & Moser 2015).

On the other hands in case of Re_τ =8000, the magnitude of the second peaks exceeds that of the first peak, but the wave-length of the second peaks normalized in outer scale are almost constant in all cases. In consequence, the plateau region become narrower compared with Re_τ=4000. The present DNS results are qualitatively consistent to the experimental results by Rosenberg et al. (2013).

The wave-length of peaks in pre-multiplied spectrum for the streamwise turbulent velocity are summarized in Table 2. The wave-lengths of the fist peak are scaled by wall-units and those normalized in outer scale are gradually decreased with increasing of Re_τ. On the other hands, the wave-lengths of the second peaks are scaled by outer scale.

Table 2. wave-length of peaks in pre-multiplied spectrum.

Re_τ	1st peak			2nd peak		
	$k_x h$	λ_x^+	λ_x/h	$k_x h$	λ_x^+	λ_x/h
1000	4.7	1337	1.3			
2000	8.6	1461	0.7	1.2	10472	5.2
4000	14.5	1733	0.4	1.2	21481	5.4
8000	27.5	1828	0.2	1.6	32016	4.0

Flow visualization

Figure 11 shows the bird- and top-view of contour plots of streamwise turbulent velocity in cases of Re_τ=1000 and 8000.

In case of Re_τ =1000, the same structures normalized in outer scale are appeared both in outer region y/h > 0.2 and overlap region y^+ =200 as shown in FIG.11-(a).

In case of Re_τ =8000, the large-scale structures normalized in outer scale can be observed in outer region y/h > 0.2. However, the streaky structures in overlap region is obviously small

compared with above large-scale structures. In near wall region y^+=9, streaky structures normalized in wall-units can be observed

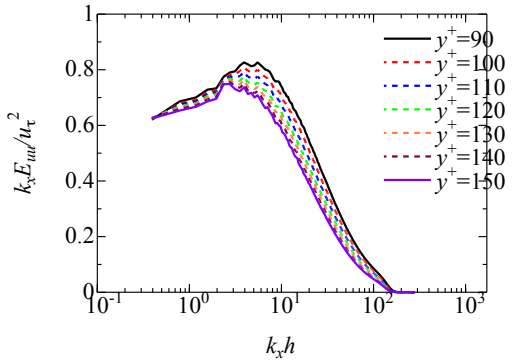

(a) Re_τ=1000

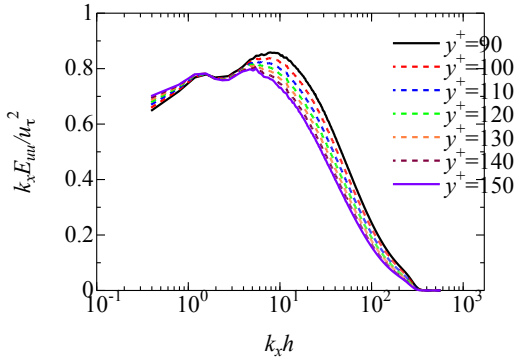

(b) Re_τ=2000

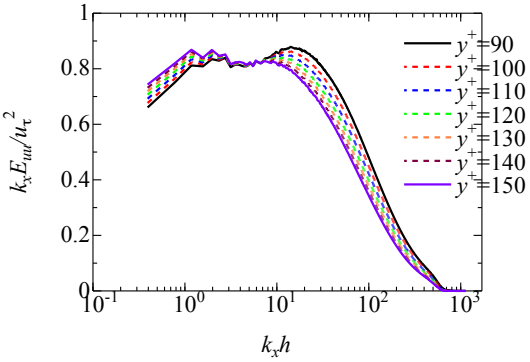

(c) Re_τ=4000

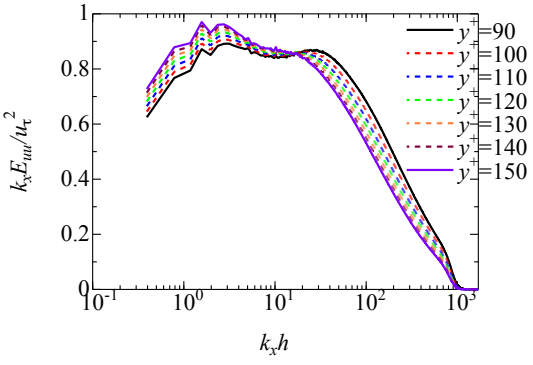

(d) Re_τ=8000

FIG. 10 Pre-multiplied spectrum of streamwise turbulent velocity at overlap region.

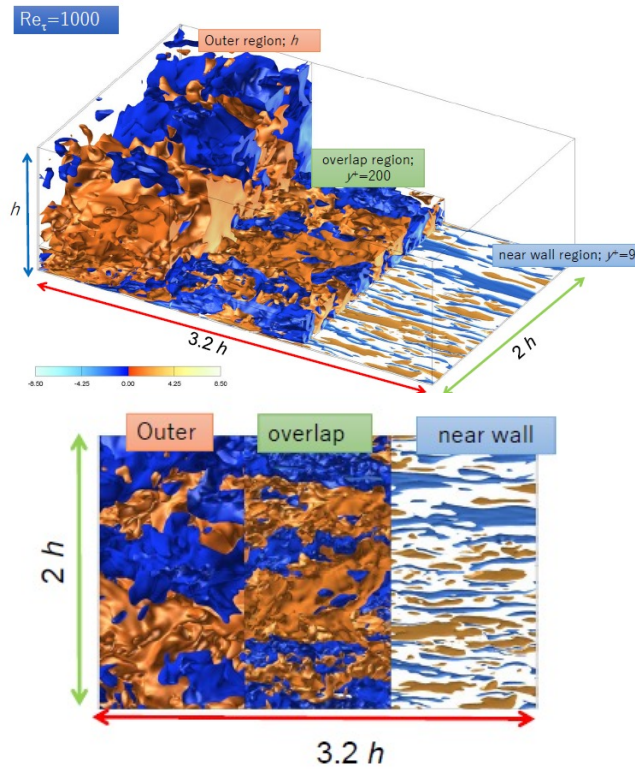

(a) Re_τ =1000

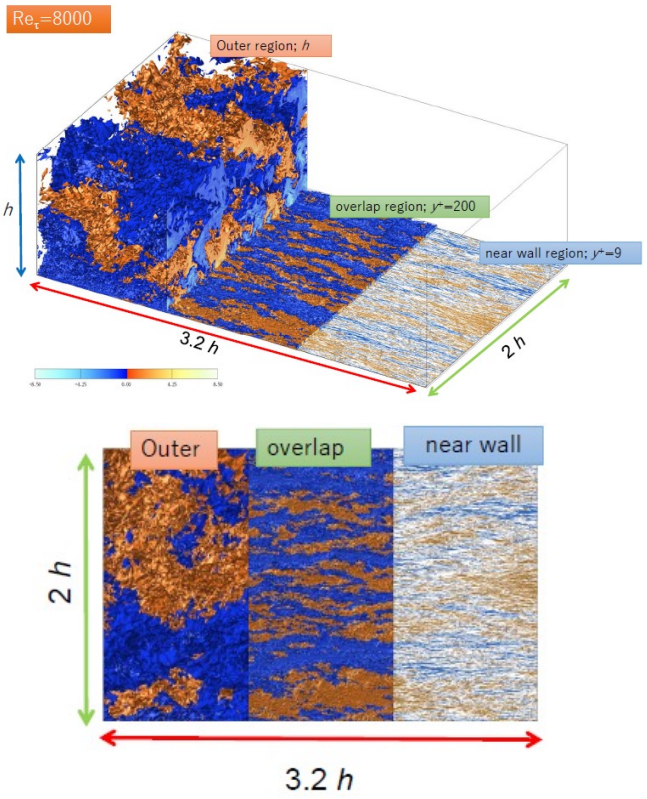

(b) Re_τ=8000

FIG.11 Contour plots of streamwise turbulent velocity, bird- and top-view cut out $3.2h \times h \times 2h$ domain, red region; high-speed, blue region; low-speed.

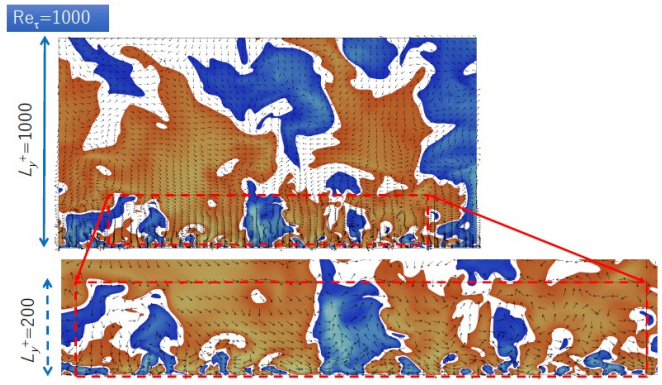

(a) Re$_\tau$ = 1000

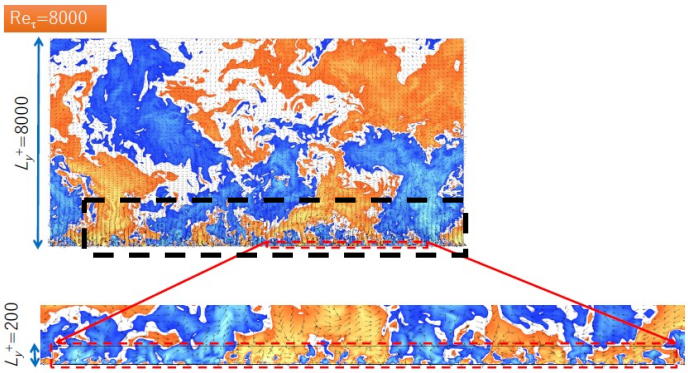

(b) Re$_\tau$ = 8000

FIG. 12 Contour plots of streamwise turbulent velocity and vector plots of spanwise and wall-normal turbulent velocities, end view cut out $3.2h \times h \times 2h$ domain, (a) Re$_\tau$ = 1000, (b) Re$_\tau$ = 8000, red region; high-speed, blue region; low-speed.

both in Re$_\tau$ =1000 and 8000. According to the bimodal peaks at low wave-number in pre-multiplied spectrum and this visualization, the intermediate scale structures between large-scale structures and primary structures near the wall will be formed for Re$_\tau$ > 4000.

Figure 12 also shows the end view of contour plots of streamwise turbulent velocity. As shown in FIG. 12-(b), interaction between the intermediate scale structures surrounded black broken-line and primary structures near the wall surrounded red-broken line is observed at the overlap region y^+=200. Furthermore, the plateau profiles of von Karman constant as shown in FIG.6 and Reynolds number effects on turbulent energy budget as shown in FIG. 9, are appeared in the same region with above intermediate scale structures for Re$_\tau$ > 4000. Therefore, the characteristics of these intermediate scale structures might be regarded as the high-Reynolds number effects.

DISCUSSION AND CONCLUSION

In this study, we carried out DNSs of turbulent channel flows up to Re$_\tau$ =8000. In streamwise pre-multiplied spectrum, the magnitude of the low wave-number peaks (2nd peaks) of Re$_\tau$=8000 exceeds that of the high wave-number peak (1st peak) as shown in FIG.10-(d). In consequence, we conclude that the plateau region corresponded to the k_x^{-1} law proposed by Perry et al. (1982) cannot be appeared in present Reynolds number ranges.

On the other hands, the wave-lengths of high-wave number peak (1st peak) are gradually decreased with increasing of Re$_\tau$ in outer scale. Thereby, the 1st and 2nd peak might keep one digit difference between high- and low-wave length in case of Re$_\tau$ =50,000. This suggests that the true plateau region in streamwise pre-multiplied spectrum might be found. However, we observed the he intermediate scale structures between large-scale structures and primary structures near the wall, and these structures will have the relationships between high Reynolds number effects in turbulent statistics at y/h < 0.2. From this view point, the true plateau region might not be found at y^+=200 but be appeared at y/h =0.2 caused by interaction between large-scale structures in outer layer and the intermediate scale structures in inner layer.

ACKNOLODGEMENT

This research used computational resources of NEC SX-ACE provided by Japan Agency for Marin-Earth Science and Technology (JAMSTEC) through the HPCI System Research project (Project ID:hp160173), and is partially supported by "Joint Usage/Research Center for Interdisciplinary Large-scale Information Infrastructures" in Japan (Project ID:jh160045-MDJ).

REFERENCS

Bernardini, M., Pirozzoli, S., & Orlandi, P., 2014, "Velocity statistics in turbulent channel flow up to Re$_\tau$ = 4000", *Journal of Fluid Mechanics*, 742, pp.171-191.

Laadhari, F., 2007, "Reynolds number effect on the dissipation function in wall-bounded flows", *Physics of Fluids*, 19(3), 038101.

Lee, M & Moser, R. D., 2015, "Direct Numerical Simulation of Turbulent Channel Flow up to Re$_\tau$=5200", *Journal of Fluid Mechanics*, 774, pp.395–415.

Lozano-Durán, A., & Jiménez, J., 2014, "Effect of the computational domain on direct simulations of turbulent channels up to Re$_\tau$= 4200", *Physics of Fluids*, 26(1), 011702.

Hoyas, S., & Jiménez, J., 2008, "Reynolds number effects on the Reynolds-stress budgets in turbulent channels", *Physics of Fluids*, 20(10), 101511.

Hutchins, N., & Marusic, I., 2007, "Evidence of very long meandering features in the logarithmic region of turbulent boundary layers", *Journal of Fluid Mechanics*, 579, pp.1-28.

Morinishi, Y., Lund, T. S., Vasilyev, O. V., & Moin, P. ,1998, "Fully conservative higher order finite difference schemes for incompressible flow", *Journal of computational physics*, 143(1), pp.90-124.

Nickels, T. B., Marusic, I., Hafez, S., & Chong, M. S., 2005, "Evidence of the k_x^{-1} law in a high-Reynolds-number turbulent boundary layer. Physical review letters, 95(7), 074501.

Perry, A. E., Henbest, S., & Chong, M. S., 1986, "A theoretical and experimental study of wall turbulence", *Journal of Fluid Mechanics*, 165, pp.163-199.

Rosenberg, B. J., Hultmark, M., Vallikivi, M., Bailey, S. C. C., & Smits, A. J., 2013, "Turbulence spectra in smooth-and rough-wall pipe flow at extreme Reynolds numbers", *Journal of Fluid Mechanics*, 731, 46-63.

Thompson, R. L., Sampaio, L. E. B., de Bragança Alves, F. A., Thais, L., & Mompean, G., 2016, "A methodology to evaluate statistical errors in DNS data of plane channel flows", Computers & Fluids, 130, 1-7.

Townsend, A. A. 1980 The structure of turbulent shear flow, 2nd edn. Cambridge University Press.

Yamamoto, Y. & Kunugi, T. 2016, "MHD effects on turbulent dissipation process in channel flows with an imposed wall-normal magnetic field", *Fusion Eng. Des.* 109-111, pp.1137-1142.